

Magnetic properties and giant magnetoresistance effect in $[\text{Fe}/\text{Pt}]_n$ granular multilayers

D. PINZARU^{a,*}, S. I. TANASE^{a,b}, P. PASCARIU^a, A. V. SANDU^c, V. NICA^a, V. GEORGESCU^a

^aFaculty of Physics, “Alexandru Ioan Cuza” University, Iasi, 700506, Romania

^b“Alexandru Cel Bun” College, Gura Humorului, 725300, Romania

^cFaculty of Materials Science and Engineering, “Gheorghe Asachi” Technical University, Iasi, 700050, Romania

We report in this paper the first observation of giant magnetoresistance as high as 23% in electrodeposited $[\text{Fe}/\text{Pt}]_n$ granular multilayers with different thicknesses of bi-layers. $[\text{Fe}/\text{Pt}]_n$ multilayers were prepared by electrodeposition, through the single bath technique. Cu (100) textured polycrystalline foils were used as substrate. The composition of the studied samples is $\text{Cu}:\text{Pt}(x \text{ nm})/[\text{Fe}(t_{\text{Fe}} \text{ nm})/\text{Pt}(x \text{ nm})]_n$, in which the thickness of the iron layer varied between 2.5÷12.5 nm while the thickness of the non-magnetic Pt layer is varied by changing the bottom Pt layer thickness x between 0.5÷3.0 nm. The SEM characterization of the multilayer revealed a granular structure of the deposit with the granule diameter in the range from 2 to 11 nm. These results are comparable with those obtained by the X-ray diffraction measurements of crystallites size obtained by the Scherer equation. The hysteresis loops showed that the magnetic properties are influenced both by the thickness of the bi-layer and by the number of periods (n). The coercivity (H_c) varied in the range 8÷21 $\text{kA}\cdot\text{m}^{-1}$ and the remanence ratio was $M/M_s = 0.23\div 0.81$. The samples display out of plane anisotropy and anti-ferromagnetic type coupling between layers, as it was emphasized by means of the torsion magnetometer. $[\text{Fe}/\text{Pt}]_n$ electrodeposited multilayers display giant magnetoresistance effect which can be explained mainly by the exchange interaction among neighbouring layers and by the spatially inhomogeneous magnetic structure of the granular multilayer (favouring spin scattering at the interfaces between grains and layers).

(Received March 4, 2011; accepted March 16, 2011)

Keywords: Fe/Pt Multilayers, Anisotropy – magnetic, Coercivity field, Magnetoresistance, Scanning electron microscopy, Torque magnetometry

1. Introduction

During the last two decades, many studies were dedicated to understanding the magnetic behaviour of the nanostructured materials (e.g., multilayers, nanowires, or granular films), which exhibit interesting magnetic and magnetoresistance properties [1]. These materials with bi-layer thickness in the nanometer range have some remarkable properties, which are unattainable in bulk materials; the major interest is represented by their magneto-transport properties – the giant magnetoresistance (GMR) effect [2]. The magnitude of GMR is influenced by many factors. It was reported that the GMR effect in multilayer changes periodically with the thickness of nonmagnetic layer [3-5], or with the thickness of the ferromagnetic layer [1, 4, 6-8]. S. Dulal [9] and I. Bakonyi [10] reported that the bi-layers number has some effect on the magnitude of GMR.

Different techniques were used to prepare multilayer on the nanometer scale and it was shown that, the physical properties depend on the production methods, however, promising results were obtained using less expensive techniques like electrochemical methods [1, 11, 12]. Multilayers produced by electrochemical route proved to be of comparable quality with those of the physical

methods. The electrodeposition of multilayers was performed using a single [13, 14] or two bath technique [15]. The use of a single bath has some advantages: it requires a simple apparatus and offers low risk of oxide formation at the fresh interface due to non-exposure to the atmosphere.

Various investigations on the development of the Fe/Pt multilayer were carried out due to its technical application (e.g., high-density recording media or micromagnets in micro-electromechanical systems). Most of these films were prepared by sputtering, vapour deposition, or laser ablation [16-19]. There are authors who reported that Fe/Pt multilayer having good magnetic properties can also be obtained by electrodeposition [20-23]. The Fe/Pt multilayers represent a particularly complicated case because depend on the multilayer periodicity [24, 25].

The aim of the present research is firstly to obtain Fe/Pt multilayers by electrodeposition, and secondly to study their magnetic and magnetoresistance properties. We prepared granular multilayer by electrodeposition and we labelled them $\text{Pt}(x \text{ nm})/[\text{Fe}(t_{\text{Fe}} \text{ nm})/\text{Pt}(x \text{ nm})]_n$. In this process of preparation, the thickness of the iron layer (t_{Fe}) varied between 2.5 and 12.5 nm and the thickness of the non-magnetic Pt layer is varied by changing the thickness

(x) of the bottom Pt layer in the range 0.5–3.0 nm. We studied the effects of both the Pt layer thickness and the ferromagnetic layer on the properties of multilayer; the effect of bi-layer number on the magnetic and transport properties was also reported. The magnetic and magnetoresistance properties of the samples were measured and discussed in correlation with their morphology.

2. Experimental

As we have already mentioned, the samples studied in this paper were prepared by electrodeposition, using a single bath method. Electrodeposition was performed in potentiostatic regime. All the depositions were made in a three-electrode cell containing iron as a counter electrode, a copper disk as a working electrode (substrate) and a platinum wire as a quasi-reference electrode. The disk-shaped cathode (20 mm in diameter) was made of (100)-textured polycrystalline copper foils. The Fe/Pt multilayers were electrolytically deposited from a solution with the following composition: $\text{Fe}(\text{NH}_4)_2(\text{SO}_4)_2 \cdot 6\text{H}_2\text{O}$ (250 $\text{g} \cdot \text{l}^{-1}$), K_2PtCl_6 (10 $\text{g} \cdot \text{l}^{-1}$), H_3BO_3 (50 $\text{g} \cdot \text{l}^{-1}$) and NaCl (20 $\text{g} \cdot \text{l}^{-1}$). We used double distilled water in obtaining every solution, and we prepared a new solution every day. The bath temperature was maintained at $24 \pm 1^\circ\text{C}$, without stirring the electrolyte, and the pH of the bath was maintained at 3.5. Before the electrodeposition, the copper substrates were mechanically polished, rinsed in acetone, washed in de-ionised water and finally activated in 10% H_2SO_4 .

Cyclic voltammetry experiments were carried out to optimize the deposition parameters for the individual Fe and Pt layers. The thicknesses of individual Fe and Pt layers, t_{Fe} and x (t_{Pt}), were estimated from the I–t curves using Faraday's laws.

The structure of the films were investigated by θ -2 θ X-ray diffraction (XRD, Shimadzu LabX XRD-6000) using $\text{CuK}\alpha$ radiation ($\lambda = 1.54 \text{ \AA}$). The morphology and the quantitative chemical composition of the samples were investigated by scanning electron microscopy (SEM/EDAX). The magnetic measurements were carried out at room temperature with an ac induction method with computerized data acquisition (frequency of 50 Hz and in a maximum field of 60 $\text{kA} \cdot \text{m}^{-1}$) and by torsion magnetometer.

The resistance (R) measurements of the samples were performed at room temperature by using four-terminal contacts applied on the film surface, using an HM 8112-2 programmable multimeter. The dc magnetic field (applied in the film plane parallel to the current, in the so called CIP longitudinal configuration) varied in the domain $\pm 400 \text{ kA} \cdot \text{m}^{-1}$. In this paper, the magnetoresistance was calculated using the equation:

$$\frac{\Delta R}{R} (\%) = \frac{R(H) - R(H_{\max})}{R(H_{\max})} \times 100, \quad (1)$$

in which $R(H)$ denotes the resistance measured in the field H and $R(H_{\max})$ defines the resistance in the maximum applied magnetic field.

3. Results and discussion

Firstly, some experiments were carried out to optimize the deposition parameters of the individual Fe and Pt layers. In order to study the nucleation and the growth mechanisms for the two basic layers that compose a multilayer, we plated films of Fe and Pt with a thickness of about 300 nm. The nominal thicknesses of individual layers, t_{Fe} and t_{Pt} , were estimated from I–t curves using Faraday's law:

$$m = \frac{ItM}{nF}, \quad (2)$$

In equation (2), m represents the weight of plated metal, I – current intensity, t – deposition time, M – weight of one mole of the metal, n – valence of the dissolved metal in solution, and F – Faraday's constant. The deposition rate of the Pt and Fe layers was 0.5 and 2.5 nm / sec.

Secondly, a series of multilayer (starting with Pt layer) of varying periods were grown, in order to study the effects of both the bi-layer thickness and the periods number on the morphology and, consequently, on the magnetic and magnetoresistance properties. The exact composition of the Fe/Pt multilayer sample is $\text{Cu}:\text{Pt}(x \text{ nm})/[\text{Fe}(t_{\text{Fe}} \text{ nm})/\text{Pt}(x \text{ nm})]_n$. The multilayer structure is shown schematically in Fig. 1.

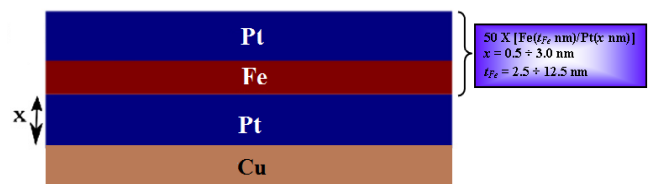


Fig. 1. Multilayer structure of Fe/Pt film.

We investigated the samples from this series, in which the thickness of the Fe varied between 2.5 and 12.5 nm and the thickness of the non-magnetic Pt layer is varied by changing the bottom Pt layer thickness x , ranged from 0.5 nm to 3.0 nm. Details of some representative samples from these series (the samples were labelled S1-S8) are presented in Table 1.

Table 1. The series of Pt(x nm)/[Fe(t_{Fe} nm)/Pt(x nm)]_n multilayer grown on Cu(100) substrate.

Sample Pt(x nm)/[Fe(t _{Fe} nm)/Pt(x nm)] _n	x (nm)	t _{Fe} (nm)	λ=t _{Fe} + x (nm)	Number of bi-layer (n)
S1	1	2.5	3.5	50
S2	1	5	6	50
S3	1	7.5	8.5	50
S4	2.5	12.5	15	50
S5	2.5	2.5	5	50
S6	2.5	5	7.5	50
S7	2.5	7.5	10	50
S8	2.5	2.5	5	100

Fig. 2 shows the XRD patterns for the sample containing only Fe and for the samples S1 Pt(1 nm)/[Fe(2.5 nm)/Pt(1 nm)]₅₀ and S2 Pt(1 nm)/[Fe(5 nm)/Pt(1 nm)]₅₀. The XRD patterns of the Fe films show that the individual layers display a *bcc* phase for Fe (111) films. The Scherrer's formula:

$$D = \frac{0.9\lambda}{\beta \cos \theta}, \quad (3)$$

was used to estimate the average crystallite size (*D*). In the equation (3), λ is the X-ray wavelength (λ = 1.54060 Å) and β denotes the broadening of the diffraction line measured at half of its maximum intensity.

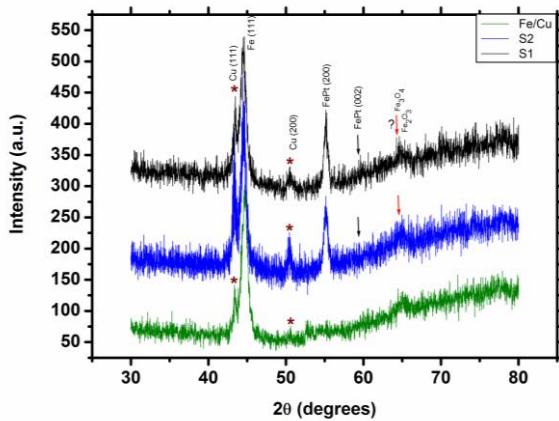


Fig. 2. XRD patterns of the Fe films and for the samples S1 Pt(1 nm)/[Fe(2.5 nm)/Pt(1 nm)]₅₀ and S2 Pt(1 nm)/[Fe(5 nm)/Pt(1 nm)]₅₀ electrodeposited onto Cu (110) substrate.

The values obtained for the crystallite size (*D*), calculated using equation 2 for Fe (111) films are of about 9 nm. The XRD patterns of the Fe/Pt multilayer indicate the formation of a disordered *fcc* FePt phase; the crystallite size for the samples S1 and S2 are of about 8 nm and of about 11 nm, respectively; one can also observe from Fig. 2 is the formation of iron oxide and, for this reason, the films prepared contain a large amount of oxygen (confirmed by SEM analysis).

Scanning electron microscopy (SEM) was employed to investigate the morphology of the films. From the SEM measurements, we found out that the surface morphology of the electrodeposited films (the shape and size of the crystallites) changes as a result of the thickness of layers. For a brief presentation of the experimental results, we chose as example SEM images for the two representative samples of this study. Fig. 3 shows the scanning electron micrographs (50 μm×50 μm) of the samples S1 (Fig. 3a, b) and S2 (Fig. 3c, d).

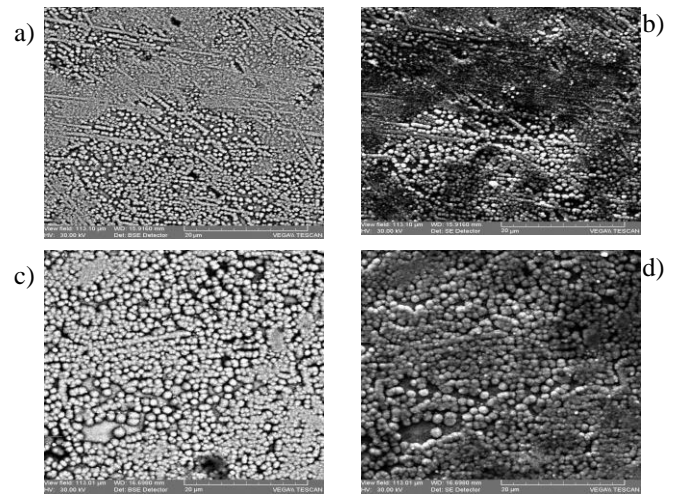


Fig. 3. SEM images for the samples S1(a, b) and S2(c, d).

In Fig. 3, the SEM images show that a granular morphology is formed in the case of both samples (S1 and S2), but Figs. 3a and 3b indicate that for the sample S1 the grain size is smaller than for the sample S2. The surface morphology of the electrodeposited multilayer is similar for our samples. The relationship between the size of the grains in granular multilayer and the nominal layer thickness is generally determined by the three-dimensional growth process. The average diameter of the grains can be much larger than the nominal layer thickness, depending on the material parameters (e.g., various electrodeposition parameters, as well as surface energy, lattice parameter, etc.) The increase of the iron layer thickness leads to the increase of the magnetic grain size and of the density of

the nanocrystalline grains as it is shown by comparison between the SEM images of the samples S1 and S2, respectively. The scanning electron micrograph images show that the samples are composed from a mixture of grains with various diameters grown from different nucleation sites onto copper support. The structure consists of many uniformly distributed grains surrounded by uncovered sites between aggregates (mainly Cu and iron oxide).

From the SEM analysis, we can notice that the Fe/Pt granular multilayer is developed by means of a Volmer–Weber mechanism. The existence of grains with varied diameters proves that the mechanism of the films grows by progressive nucleation.

We have also found from the SEM experiments, that when the thickness of the Fe layer is increased, higher oxygen content is included in the deposit. As an example, in the case of the sample S2 more oxygen (28.73 at. %) is included in comparison with the oxygen content in the case of the sample S1 (where the oxygen content is 20.14 at. %). We suggest the following explanation for this high oxygen content in our samples: Pt favours the hydrogen evolution and, in turn, the formation of iron oxide and iron

hydroxide and by this reason the films we prepared contain a large amount of oxygen. During the multilayer electrodeposition, the less noble metal tends to dissolve during the deposition of the more noble metal. For the deposition of a Pt-rich layer with low oxygen content, the potential should be chosen as positive as possible, as the oxygen (and iron) incorporation increases for more negative potentials. The upper limit is given by the start of Fe dissolution from a previously deposited Fe-rich layer. Further work is required in order to clarify this variation of the oxygen content in the multilayer, which is, however, not the focus of the present paper.

The magnetic properties of the $[\text{Fe}/\text{Pt}]_n$ multilayer have been investigated by an *ac* method with computerized data acquisition and torque measurements. We found out that the magnetic behaviour is influenced both by the thickness and by the number of bi-layers (n). A comparison between the hysteresis loops of the studied samples is presented in Fig. 4. The measured coercivity (H_c) of the samples varied between $8.39 \text{ kA}\cdot\text{m}^{-1}$ for the sample S8 and $12.37 \text{ kA}\cdot\text{m}^{-1}$ for the sample S1, while the remanence ratio (M/M_s) is of 0.23 and 0.81, respectively.

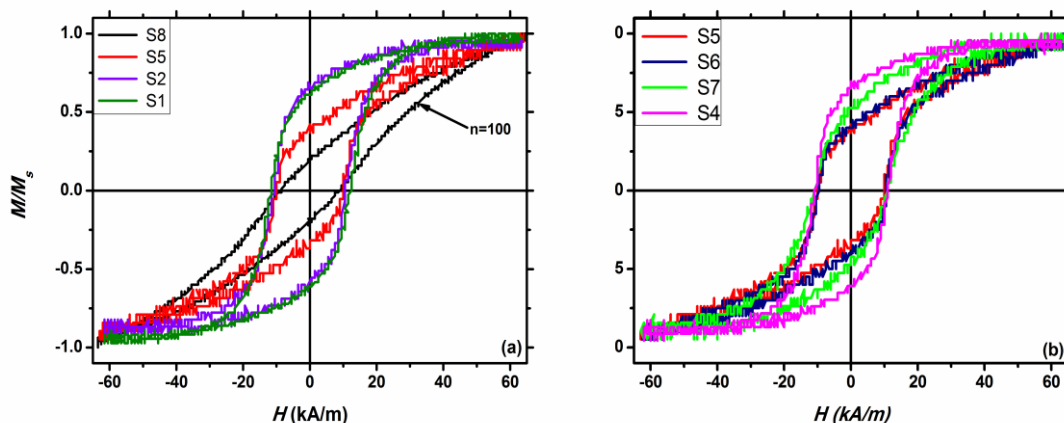


Fig. 4. Comparison between the hysteresis loops recorded for the $\text{Pt}(x \text{ nm})/[\text{Fe}(t_{\text{Fe}} \text{ nm})/\text{Pt}(x \text{ nm})]_n$ multilayer.

From the magnetic measurements, we found that the magnetization is in the plane of the layers and anti-ferromagnetic (AF) coupling between the adjacent Fe layers is found when the Pt thickness t_{Pt} is smaller than 3.0 nm and the number of bi-layers is 100 (Fig. 3a). As the thickness of both Fe and Pt layer decreases below 12.5 nm and 3.0 nm, respectively, the hysteresis loop is progressively tilted. When the applied field is decreased to zero, the AF coupling brings the magnetization back to about zero. As it can be seen from Fig. 3a, the AF coupling increases when the number of bi-layers increases from 50 to 100, and also when the t_{Fe} decreases from 12.5 nm to 2.5 nm. The existence of such AF coupling has already been found in Fe/Cr sandwiches by Grünberg [26, 27] and Carbone [28] and their co-workers.

The shapes of the magnetic susceptibility curves are different for the studied samples as a function of the thickness and number of bi-layer (Fig. 5). In Fig. 5, one can observe that each curve has its specific shape.

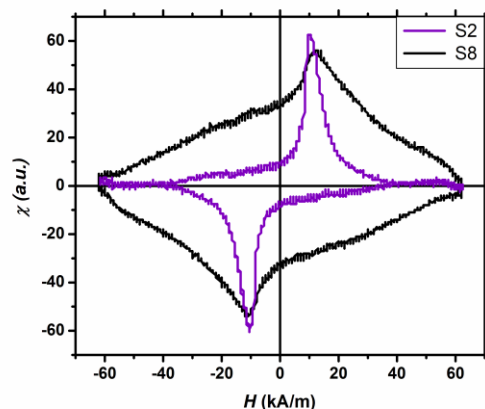


Fig. 5. Magnetic susceptibility curves for the samples S2 $\text{Pt}(1 \text{ nm})/[\text{Fe}(5 \text{ nm}/\text{Pt}(1 \text{ nm})]_{50}$ and S8 $\text{Pt}(2.5 \text{ nm})/[\text{Fe}(2.5 \text{ nm}/\text{Pt}(2.5 \text{ nm})]_{100}$.

The magnetic properties of the samples were also investigated by means of torque magnetometry, at room temperature. Fig. 6(a-c) shows the torque curves taken for rotations of increasing and decreasing angles of θ for the samples S1 Pt(1 nm)/[Fe(2.5 nm)/Pt(1 nm)]₅₀, S2 Pt(1 nm)/[Fe(5 nm)/Pt(1 nm)]₅₀ and S8 Pt(2.5 nm)/[Fe(2.5 nm)]₁₀₀, respectively. The film plane was perpendicularly oriented to the field-rotation plane, e. g. the torque was measured around an arbitrary axis parallel to the film plane, starting from the plane of the film ($\theta = 0$). The applied magnetic field was of $15 \text{ kA}\cdot\text{m}^{-1}$, $20 \text{ kA}\cdot\text{m}^{-1}$, and $28 \text{ kA}\cdot\text{m}^{-1}$.

As the applied field increases, the torque curves become asymmetric, i.e. the rotational loss appears and it

is measurable from the area enclosed by the clockwise (0-360°, labelled F) and anticlockwise (360°-0, labelled B) curves. For fields exceeding the anisotropy field, the torque curves are proportional to $\sin 2\theta$. This behaviour can be ascribed to the anti-ferromagnetic type interlayer coupling for the samples. The experimental torque curves exhibit mainly a two-fold symmetry with a positive slope of $\theta=0^\circ$ and a negative slope around $\theta=90^\circ$. This indicates that the easy magnetisation direction is perpendicular ($\theta=90^\circ$) to the film plane. The proportionality between the torque L and the $\sin \theta$ which occurs at relatively low fields for the samples can be accounted for the presence of anti-ferromagnetic type coupling between Fe layers.

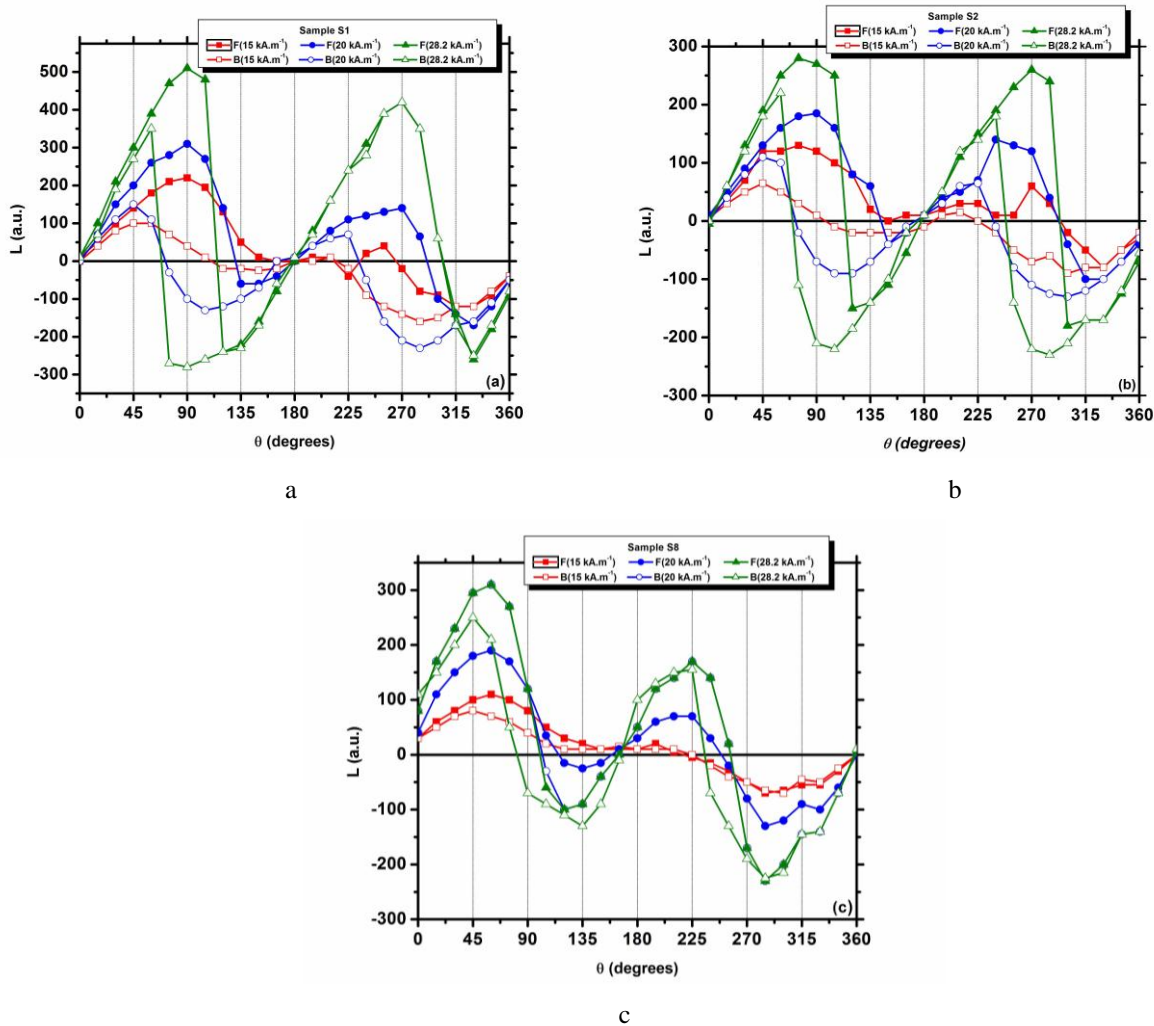


Fig. 6. Torque curves for the sample S1 (a), S2 (b) and S8 (c), plotted from 0 to 360 degrees (F) and from 360 to 0 degrees (B). The torque curves were measured for the fields: $15 \text{ kA}\cdot\text{m}^{-1}$, $20 \text{ kA}\cdot\text{m}^{-1}$ and $28 \text{ kA}\cdot\text{m}^{-1}$.

The torque measurements of ferromagnets in high magnetic fields show no rotational hysteresis because the hysteresis always results from irreversible magnetization changes, which are not possible in a sufficiently high saturated magnetic field. We can explain the increase of the energy loss with an applied magnetic field in our experiments by analogy with the results obtained in references [29, 30]. In their experiments, Meiklejohn and

Bean [29, 30] proved that the torque measurements of the ferromagnets in high magnetic fields show no rotational hysteresis because the hysteresis results always from irreversible magnetization changes, which are not possible in a sufficiently high saturated magnetic field. In a sufficiently high magnetic field, the experiments showed an appreciable hysteresis of the torque indicating that the magnetic state of (part of) the sample changed irreversibly

when rotating the film in a magnetic field. The energy dissipated per revolution is equal to the difference between the areas of F and B curves. We consider that the $\sin \theta$ shape of the torque curve in low fields and the increase of the hysteresis losses in higher magnetic field are the evidence for the anti-ferromagnetic type coupling in Fe/Pt multilayer. The difference in torque values, representing the rotational hysteresis, is also shown in Fig. 7.

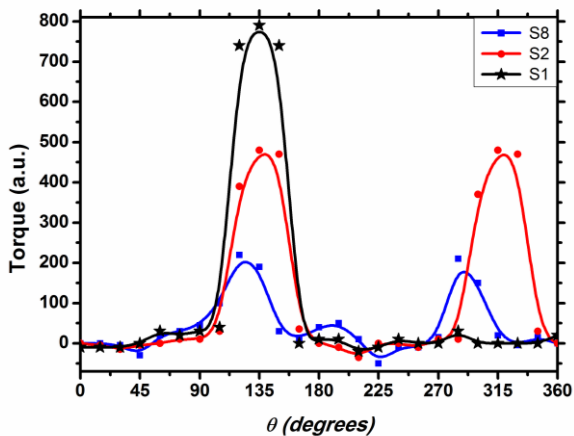


Fig. 7. Rotational hysteresis of Fe/Pt multilayers.

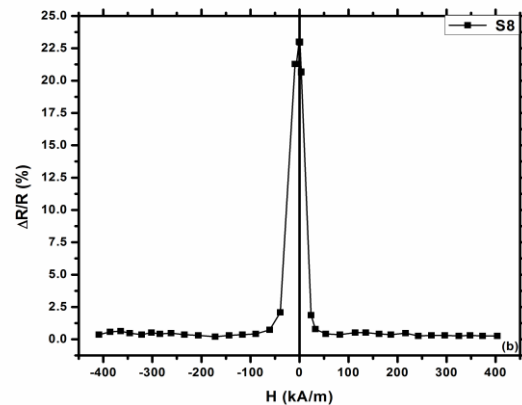
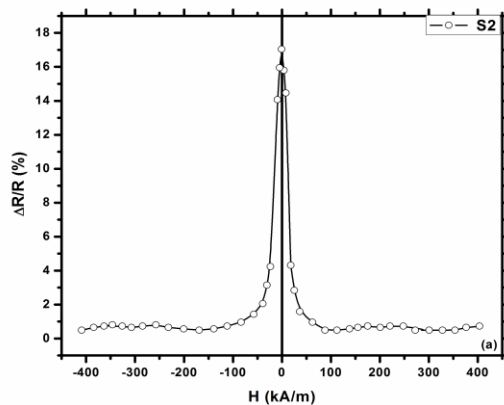


Fig. 8. Magnetoresistance ($\Delta R/R$) for the samples S2 Pt(1 nm)/[Fe(5 nm)/Pt(1 nm)]₅₀ (a) and S8 Pt(2.5 nm)/[Fe(2.5 nm)/Pt(2.5 nm)]₁₀₀ (b) as a function of applied magnetic field H (kA/m).

The enhancement of the magnetoresistance can be attributed to the spatially inhomogeneous magnetic structure having different magnetic component and to the exchange interaction between neighbouring layers (as it results from the magnetic measurements). These effects depend on the polarization processes acting on the spin of conduction electrons, as well as on the magnetic configuration of the system. In addition, the thickness of the Pt interlayer has an important role in the diffusion and transportation processes.

4. Conclusions

We prepared by electrochemical method granular Fe/Pt multilayer with extremely thin bi-layer thickness (nominal period varied in the range 3.5-15.0 nm) on Cu (100) substrate. The Fe/Pt multilayer was deposited from a

single sulphate bath in potentiostatic regime. We found out that the crystalline structure and magnetic properties of the film are strongly influenced by the bi-layer thickness and by the period number.

It is very possible that the increase of the coercivity and rotational hysteresis are different manifestations of the same effect, i.e. the losses produced during the rotation of the ferromagnetic (FM) layer by the AFM spin drag. We can conclude from these experiments that a decreasing of non-magnetic and ferromagnetic layer thickness results in increasing the strength of the interaction between magnetic layers. In addition, the interface number should have some effect on the magnitude of the interaction between magnetic layers.

The measurements of resistance versus the applied *d.c.* magnetic field were performed at room temperature by using the device described in the experimental part of the paper. We have found that GMR effect in CIP configuration varied between 17% and 23% as a function of the thickness and number of bi-layer. The variation of giant magnetoresistance with an applied magnetic field for the samples S2 Pt(1 nm)/[Fe(5 nm)/Pt(1 nm)]₅₀ and S8 Pt(2.5 nm)/[Fe(2.5 nm)/Pt(2.5 nm)]₁₀₀ are presented in Fig. 8. For this samples, the contribution of the giant magnetoresistance is of 17% in the case of sample S2 Pt(1 nm)/[Fe(5 nm)/Pt(1 nm)]₅₀ and 23% in the case the samples S8 Pt(2.5 nm)/[Fe(2.5 nm)/Pt(2.5 nm)]₁₀₀, respectively.

The experimental results show that the anti-ferromagnetic coupling between the adjacent Fe layers appears when the Pt thickness t_{Pt} is smaller than 3.0 nm and the number of bi-layers increases from 50 to 100; the coercivity varied between $8 \div 21 \text{ kA} \cdot \text{m}^{-1}$, while the remanence ratio varied in the range $0.23 \div 0.81$. From the torque measurements, we can conclude that when the applied magnetic field increases, the curves become asymmetric and the rotational loss appears. For fields exceeding the anisotropy field, the torque curves become symmetric and irreversible. This behaviour can be ascribed to the anti-ferromagnetic type interlayer coupling between adjacent Fe layers.

Experimental results show that the giant magnetoresistance of [Fe/Pt]_n multilayers increases with the increase of bi-layer number. The giant magnetoresistance contribution is of

23% for the multilayer consisting of 100 bi-layers (Pt(2.5 nm)[Fe(2.5 nm)/Pt(2.5 nm)]₁₀₀) and of about 17% for the samples consisting of 50 bi-layers (Pt(1 nm)[Fe(5 nm)/Pt(1 nm)]₅₀).

Acknowledgements

This work was supported by the Ministry of Education, Research, Youth and Sport and by the Social European Funds under Project No. RO08- POSDRU-6/1.5/S/25 and by grant POSDRU/89/1.5/S/49944.

References

- [1] I. Bakonyi, L. Péter, *Progress in Materials Science* **55**, 107 (2010).
- [2] K. Ludwig, J. Hauch, R. Mattheis, K. U. Barholz, G. Rieger, *Sens. Actuators A* **106**, 15 (2003).
- [3] S. Kashiwabara, Y. Jyoko, Y. Hayashi, *Physica B* **249**, 47 (1997).
- [4] D. K. Pandya, P. Gupta, S. C. Kashyap, S. Chaudhary, *J. Magn. Magn. Mater.* **321**, 974 (2009).
- [5] I. Bakonyi, E. Simon, B. G. Toth, L. Péter, L. F. Kiss, *Phys. Rev. B* **79**, 174421/1-13 (2009).
- [6] Th. Eckl, G. Reiss, H. Bruckl, H. Hoffmann, *J. Appl. Phys.* **75**, 362 (1994).
- [7] S. K. J. Lenczowski, C. Schonenberger, M. A. M. Gijs, W. J. M. de Jonge, *J. Magn. Magn. Mater.* **148**, 455 (1995).
- [8] C. Christides, S. Logothetidis, M. Gioti, S. Stergioudis, S. Stavroyiannis, D. Niarchos, *J. Appl. Phys.* **83**, 7757 (1998).
- [9] S. M. S. I. Dulal, E. A. Charles, *J. Phy. Chem. Solids* **71**, 309 (2010).
- [10] I. Bakonyi, J. Tóth, L. Goulou, T. Becsei, E. Tóth-Kádár, W. Schwarzacher, G. Nabiyouni, *J. Electrochem. Soc.* **149**, C195 (2002).
- [11] M. Georgescu, V. Georgescu, *Surf. Sci.* **507–510**, 507 (2002).
- [12] S. K. Ghosh, P. Choudhury, S. K. Gupta, G. Ravikumar, M. S. Kumar, D. K. Aswal, R. O. Dusane, A. K. Grover, *Appl. Phys. Lett.* **89**, 132507 (2006).
- [13] D. S. Lashmore, M. P. Dariel, *J. Electrochem. Soc.* **135**, 1218 (1988).
- [14] D. M. Tench, J. T. White, *J. Electrochem. Soc.* **138**, 3757 (1991).
- [15] A. S. M. A. Haseeb, J. P. Celis, J. R. Roos, *J. Electrochem. Soc.* **141**, 230 (1994).
- [16] Francesca Casoli, Franca Albertini, Luigi Pareti, Simone Fabbri, Lucia Nasi, Claudio Bocchi, Roberta Ciprian, *IEEE Trans. Mag.* **41**(10), 3877-3879 (2005).
- [17] Y. H. Huang, Y. Zhang, G. C. Hadjipayanis, D. Weller, *J. Applied Physics* **93**(10), 7172 (2003).
- [18] T. Shima, K. Takanashi, Y. K. Takahashi, K. Hono, *Appl. Phys. Lett.* **81**, 1050 (2002).
- [19] Jhy-Chau Shih, Hsin-Hsin Hsiao, Jai-Lin Tsai, Tsung-Shune Chin, *IEEE Trans. Mag.* **37**, 1280 (2001).
- [20] K. Leistner, E. Backen, B. Schüpp, M. Weisheit, L. Schultz, H. Schlörb, S. Fähler, *J. Appl. Phys.* **95**, 7267 (2004).
- [21] K. Leistner, J. Thomas, H. Schlörb, M. Weisheit, L. Schultz, S. Fähler, *Appl. Phys. Lett.* **85**, 3498 (2005).
- [22] Y. Gu, D. Zhang, X. Zhan, Z. Ji, Y. Zhang, *J. Magn. Magn. Mater.* **299**, 392 (2006).
- [23] K. Leistner, S. Oswald, J. Thomas, S. Fähler, H. Schlörb, L. Schultz, *Electrochimica Acta* **52**, 194 (2006).
- [24] S. C. Chou, C. C. Yu, Y. Liou, Y. D. Yao, D. H. Wei, T. S. Chin, M. F. Tai, *J. Appl. Phys.* **95**, 7276 (2004).
- [25] Bo Yao, Kevin R. Coffey, *J. Magn. Magn. Mater* **320**, 559 (2008).
- [26] P. Grünberg, R. Schreiber, Y. Pang, M. B. Brodsky, H. Sowers, *Phys. Rev. Lett.* **57**, 2442 (1986).
- [27] F. Saurenbach, U. Walz, L. Hinchey, P. Grünberg, W. Zinn, *J. Appl. Phys.* **63**, 3473 (1988).
- [28] C. Carbone, S. F. Alvarado, *Phys. Rev. B* **36**, 2433 (1987).
- [29] W. H. Meiklejohn, C. P. Bean, *Phys. Rev.* **102**(5), 1413 (1956).
- [30] W. H. Meiklejohn, C. P. Bean, *Phys. Rev.* **105** (3), 904 (1957).

*Corresponding author: dumitritatanase@yahoo.com